

# Quantum Approximate Optimization Algorithm for PD-NOMA User Pairing

Qiwei Xiang

College of Mechanical and Electrical  
Engineering  
Sichuan Agricultural University  
Ya'an, China  
2020317018@stu.sicau.edu.cn

Yau Hee Kho

School of Engineering and Computer  
Science  
Victoria University of Wellington  
Wellington 6140, New Zealand  
yauhee.kho@vuw.ac.nz

Winston K.G. Seah

School of Engineering and Computer  
Science  
Victoria University of Wellington  
Wellington 6140, New Zealand  
winston.seah@ecs.vuw.ac.nz

Yue Tian

Fujian Key Laboratory of  
Communication Network and  
Information Processing  
Xiamen University of Technology  
Xiamen 361024, China.  
yue.tian.xmut@outlook.com

Rui Fang

College of Mechanical and Electrical  
Engineering  
Sichuan Agricultural University  
Ya'an, China  
2020217009@stu.sicau.edu.cn

\*Peng Huang

Corresponding author: College of  
Mechanical and Electrical Engineering  
Sichuan Agricultural University  
Ya'an, China  
hpsjdyd@sicau.edu.cn

**Abstract**—This work proposes the utilization of the quantum approximate optimization algorithm (QAOA) for user pairing in non-orthogonal multiple access (NOMA). By exploiting quantum concepts such as the quantum adiabatic theorem, a user pairing solution was derived that approximates a suboptimal sum rate. Moreover, an improved-QAOA is proposed to further enhance the performance by reducing the number of users in the cluster by dividing it into more clusters. Simulation results have demonstrated that the improved-QAOA yields a higher average achievable sum rate when compared to QAOA, and its solution is closer to the theoretical optimal value obtained by a brute-force enumeration method.

**Keywords**—Quantum approximate optimization algorithm, Non-orthogonal multiple access, 5G, Wireless communications, User pairing

## I. INTRODUCTION

As an emerging key technology of 5G/6G communication systems, non-orthogonal multiple access (NOMA) is becoming an important technique to improve the spectral efficiency of the system and can provide technical support for multiplying the number of user accesses [1-3]. In power domain (PD)-NOMA, signal transmission is performed by allocating different levels of power to different users and superimpose the transmitted signals, such that the superimposed signals of other users are regarded as interferences at the receiving ends. Successive interference cancellation (SIC) is used to eliminate the other interfering signals and decode the desired user's own signal [4]. As the number of users increases, too many users are multiplexed on the same subcarrier, resulting in an increase in the complexity of SIC and the degradation in error caused by SIC for the weaker users. Therefore, reducing the number of superimposed users by adopting multiple grouping methods, that is, user pairing, has become a conventional solution [5,6].

In this paper the quantum approximation optimization algorithm (QAOA) [17] has been used to solve the user pairing problem of a multi-carrier NOMA downlink scenario where it is usually regarded as a non-convex problem, so artificial intelligence methods using similar heuristics have been investigated [7-14]. However, as the number of users increases, the time complexity brought by the heuristic algorithms will also increase significantly. Introducing QAOA to the user pairing problem, the advantages of its parallelism and acceleration are expected to provide a new

paradigm for solving the problem. In most of the existing literatures, QAOA is usually used to solve mathematical problems such as MAX-Cut, MIS, etc. [15-17], while the application scenarios in specific fields, especially in wireless communications, are introduced too little [19]. To the best of our knowledge, this paper is the first that has applied QAOA to the NOMA user pairing scenario.

The main contributions of this paper are as follows:

- The NOMA downlink user pairing problem is transformed into a mathematical model of combinatorial optimization problem, and each sub-problem is abstracted as a bipartite graph, where the weights of the bipartite graph are set according to the channel gains. Then, with the goal of maximizing the overall sum rate of the system, the QAOA is used to obtain the user grouping scheme.
- With the increase of users, the number of users in each of the two groups obtained using the above-mentioned QAOA increases, and the spectral efficiency of the overall system will decrease. Therefore, in order to obtain a larger system capacity, this paper has proposed an improved-QAOA which can create more groups.

## II. SYSTEM MODEL OF A NOMA DOWNLINK

This paper considers a multi-carrier NOMA downlink as a system model. In such a scenario, the base station (BS) is assumed to locate in the middle of a single cell, which is serving  $N$  users. In order to facilitate subsequent user pairing, the number of users is set to an even number  $N=2K$ , where  $K \in \{1,2,3,\dots\}$ . The users in the cell are divided into multiple groups which are not necessarily mutually exclusive. The users within one group are allocated to the same subcarrier, and intragroup interference is mitigated by using the NOMA principle. The communication link between the users and the BS is assumed to be a zero-mean Rayleigh fading channel. The distance between BS and the  $n$ th user is presented as  $d_n$  where the channel gains is represented as  $|h_n|^2$ . In our scenario,  $\sqrt{d^{-L}}$  is assumed to be the channel pathloss where the pathloss exponent,  $L = 4$  [1,18].

In NOMA, the BS allocates different powers to the two users on the same subcarrier, and transmits by superimposing

the signals of the two users. The superimposed signal sent by the base station on each subcarrier is:

$$s_k = \sqrt{p_k} \sum_{i=1}^n \sqrt{\alpha_i} * x_i \quad (1)$$

where  $p_k$  represents the power allocated to the  $k$ th subcarrier,  $\alpha_i$  and  $i$  represent the power coefficient and transmitted signal of  $i$ th user in the subcarrier, respectively. In addition,  $\alpha_1$  and  $\alpha_2$  satisfy the constraint such that  $\alpha_1 + \alpha_2 = 1$ .

The signal received by the UE on the subcarrier is:

$$\begin{aligned} y_{k,1} &= h_1 * s_k + \sigma_1 \\ &= h_1 * \sqrt{p_k} (\sqrt{\alpha_1} * x_1 + \sqrt{\alpha_2} * x_2) + \sigma_1 \\ &= \underbrace{h_1 * \sqrt{p_k} * \sqrt{\alpha_1} * x_1}_{\text{desired \& dominating}} + \underbrace{h_1 * \sqrt{p_k} * \sqrt{\alpha_2} * x_2}_{\text{interference \& low power}} + \underbrace{\sigma_1}_{\text{noise}} \end{aligned} \quad (2)$$

$$\begin{aligned} y_{k,2} &= h_2 * s_k + \sigma_2 \\ &= h_2 * \sqrt{p_k} (\sqrt{\alpha_1} * x_1 + \sqrt{\alpha_2} * x_2) + \sigma_2 \\ &= \underbrace{h_2 * \sqrt{p_k} * \sqrt{\alpha_1} * x_1}_{\text{interference \& dominating}} + \underbrace{h_2 * \sqrt{p_k} * \sqrt{\alpha_2} * x_2}_{\text{desired \& low power}} + \underbrace{\sigma_2}_{\text{noise}} \end{aligned} \quad (3)$$

where  $h_1$  and  $\sigma_1$  are the channel gain and additive white Gaussian noise (AWGN) corresponding to the user with higher power, respectively. Similarly,  $h_2$  and  $\sigma_2$  are the channel conditions corresponding to the lower power user and the additive white Gaussian noise, respectively.

In each subcarrier, the user with the higher power will regard the signal of the user with the lower power as interference, so the signal of the user with the higher power can be directly decoded. For users with lower power, it is necessary to perform SIC to eliminate signals with higher power first, that is, first decode the received signals to obtain the signals of users with higher power. The signal of the stronger user is then subtracted from the received signal. Finally decode the remaining signal to get its own signal. In addition, it should be noted that the signal  $x$  is a normalized signal. According to Shannon's formula, the rate that can be achieved by two users in a subcarrier is:

$$R_{k,1} = \log_2 \left( 1 + \frac{|h_1|^2 * p_k * \alpha_1}{|h_1|^2 * p_k * \alpha_2 + \sigma_1^2} \right) \quad (4)$$

$$R_{k,2} = \log_2 \left( 1 + \frac{|h_2|^2 * p_k * \alpha_2}{\sigma_2^2} \right) \quad (5)$$

and the total rate that the whole system can achieve is:

$$R_{tot} = \sum_{k=1}^K (R_{k,1} + R_{k,2}) \quad (6)$$

### III. QUANTUM APPROXIMATE OPTIMIZATION ALGORITHM FOR USER PAIRING IN NOMA

QAOA is a polynomial-time algorithm based on adiabatic quantum computing algorithms. This algorithm is a "good" solution for finding optimization problems. The interpretation of this statement is that, for a given NP-Hard problem, the algorithm solves each problem instance with some quality guarantee expected, where the quality factor is the ratio between the quality of the polynomial-time solution and the quality of the true solution. One reason the QAOA algorithm is interesting is its potential to demonstrate quantum supremacy [17]. Combinatorial optimization problems

In the original QAOA version, the MAX-CUT problem which is also a combinatorial optimization problem, is used as the first problem described by QAOA. The objective function of the combinatorial optimization problem is defined as the maximum number of clauses satisfying a specific bit string.

$$C(z) = \sum_{m=1}^M C_m(z) \quad (7)$$

where  $z = z_1, z_2, \dots, z_n$  is the bit string and  $C(z) = 1$  if  $z$  satisfies clause  $M$ , and 0 otherwise [17].

#### A. The Quantum Adiabatic Theorem

In the scenario described by quantum mechanics, we describe the evolution of the state of the system by the Schrödinger equation:

$$i \frac{d}{dt} |\psi(t)\rangle = H(t) |\psi(t)\rangle \quad (8)$$

where the Dirac symbol  $|\psi(t)\rangle$  describes the state of the system at time  $t$ , and  $H(t)$  is the system Hamiltonian at that time, which expresses all possible states of the system at this moment [20]. The evolution of a closed quantum system can be described by a unitary transformation,

$$|\psi(T)\rangle = U(T, t_0) |\psi(t_0)\rangle \quad (9)$$

where  $U(T, t_0)$  represents the unitary operator from  $t_0$  to  $T$ , and  $|\psi(t_0)\rangle$  and  $|\psi(T)\rangle$  represent the wave function at two time instances.

The quantum adiabatic theorem can be briefly summarized as follows: given a Hamiltonian at time  $t=0$ , the system starts to evolve from an eigenstate of the Hamiltonian. If the system evolves slowly enough, when the evolution ends, the Hamiltonian evolves into  $H(T)$ , and the system will be approximated by this eigenstate of the Hamiltonian. Its evolution operator satisfies:

$$U(T, t_0) = e^{-i\theta \int_{t_0}^T H(t) dt} \quad (10)$$

#### B. Quantum approximate optimization algorithm (QAOA)

QAOA is a quantum algorithm based on the quantum adiabatic algorithm. By setting an appropriate initial Hamiltonian and passing through a specific quantum circuit, it evolves to the ground state, i.e. a solution, corresponding to the problem Hamiltonian [17]. In QAOA, we denote each clause by a Hamiltonian. Combined with the expression form (7), the purpose of the MAX-CUT problem in QAOA is to find a bit string  $z$  that maximizes the Hamiltonian, even if the following formula is maximized:

$$H_p(z) = \sum_{\alpha=1}^V H_\alpha(z) \quad (11)$$

In quantum mechanics, we use Dirac notation to express it. Then the above bit string is expressed as  $|00\rangle, |01\rangle, |10\rangle, |11\rangle$ , we call it a qubit string. For any string of qubits is the Kronecker product of each qubit in it. For example,  $|01\rangle = |0\rangle \otimes |1\rangle$ ,  $\otimes$  means Kronecker product, where  $|0\rangle$  and  $|1\rangle$  represent the two fundamental states that each qubit, and its mathematical form is  $|0\rangle = [1 \ 0]^T$ ,  $|1\rangle = [0 \ 1]^T$ . So  $|00\rangle$  can be expressed as  $|00\rangle = [1 \ 0 \ 0 \ 0]^T$ .

We define the sub-Hamiltonian of the MAX-CUT problem as:

$$H_\alpha = \begin{bmatrix} -1 & 0 & 0 & 0 \\ 0 & 1 & 0 & 0 \\ 0 & 0 & 1 & 0 \\ 0 & 0 & 0 & -1 \end{bmatrix}, \alpha \in V \quad (12)$$

According to formula (10), the unitary operator corresponding to the Hamiltonian can be deduced:

$$\begin{aligned}
U_{H_\alpha} &= e^{-i\theta H_\alpha} \\
&= e^{-i\theta \left( \frac{\sigma_0^{\otimes 2} - \sigma_3^i \otimes \sigma_3^j}{2} \right)} \\
&= e^{-i\theta \frac{\sigma_0^{\otimes 2}}{2}} * e^{i\theta \left( \frac{\sigma_3^i \otimes \sigma_3^j}{2} \right)} \quad (13)
\end{aligned}$$

where  $\sigma_0$  and  $\sigma_3$  represent the Pauli 0 matrix and the Pauli 3 matrix, respectively.  $i$  and  $j$  represent the two vertices of the edge respectively. Next, the second term on the right-hand side of (13) is derived:

$$\begin{aligned}
e^{i\theta \left( \frac{\sigma_3^i \otimes \sigma_3^j}{2} \right)} &= \begin{bmatrix} e^{i\frac{\theta}{2}} & 0 & 0 & 0 \\ 0 & e^{-i\frac{\theta}{2}} & 0 & 0 \\ 0 & 0 & e^{-i\frac{\theta}{2}} & 0 \\ 0 & 0 & 0 & e^{i\frac{\theta}{2}} \end{bmatrix} \\
&= \begin{bmatrix} 1 & 0 & 0 & 0 \\ 0 & 1 & 0 & 0 \\ 0 & 0 & 0 & 1 \\ 0 & 0 & 1 & 0 \end{bmatrix} \begin{bmatrix} e^{i\frac{\theta}{2}} & 0 & 0 & 0 \\ 0 & e^{-i\frac{\theta}{2}} & 0 & 0 \\ 0 & 0 & e^{-i\frac{\theta}{2}} & 0 \\ 0 & 0 & 0 & e^{i\frac{\theta}{2}} \end{bmatrix} \begin{bmatrix} 1 & 0 & 0 & 0 \\ 0 & 1 & 0 & 0 \\ 0 & 0 & 0 & 1 \\ 0 & 0 & 1 & 0 \end{bmatrix} \\
&= CNOT * (\sigma_0 \otimes RZ(-\theta)) * CNOT \quad (14)
\end{aligned}$$

Hence it could be deduced that  $U_{H_\alpha}$  is composed of *CNOT* gates and *RZ* gate, and contains an undetermined parameter,  $\theta$ .

According to (11), the unitary operator  $U_{H_p}$  corresponding to the Hamiltonian of the problem can be obtained as:

$$U_{H_p} = \prod_{\alpha=1}^V U_\alpha, \alpha \in V \quad (15)$$

where it is usual to start with the superposition state created by the Hadamard gate, *H*, which corresponds to an initial Hamiltonian  $H_0$  that is easy to construct:

$$H_0 = \sigma_1^{\otimes n} \quad (16)$$

where  $n$  represents the number of qubits used. Similar to (13), the unitary operator corresponding to the initial Hamiltonian can be derived as:

$$\begin{aligned}
U_{H_0} &= e^{-i\theta H_0} \\
&= e^{-i\theta \sigma_1^{\otimes n}} \\
&= RX(2\theta)^{\otimes n} \quad (17)
\end{aligned}$$

Hence by derivation,  $U_{H_0}$  is composed of a series of *RX* gates and also contains the undetermined parameter,  $\theta$ .

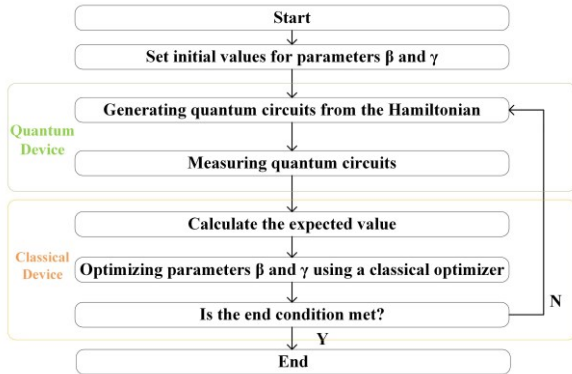


Fig. 1. Flowchart of QAOA where the QAOA algorithm is a combination of quantum computing and classical computing.

The following section completes the quantum part of QAOA, as shown in the Fig. 1, and obtains the quantum circuit of QAOA, and two unitary operators  $U_{H_p}$  and  $U_{H_0}$  with undetermined parameters where they are represented by  $\gamma$  and  $\beta$ , respectively. To complete the entire process of QAOA, an optimizer needs to be utilised so as to optimize these two pending parameters. The loss function of the optimizer in terms of the expected value of the Hamiltonian of the problem is expressed as:

$$LOSS = \langle \varphi | H_p | \varphi \rangle \quad (18)$$

where  $|\varphi\rangle$  represents the execution result of the quantum circuit; for  $\langle \varphi |$ , it has the following definition:  $\langle \varphi | = |\varphi\rangle^\dagger$  where the  $\dagger$  represents conjugate transpose. (18) represents how well the result of the quantum circuit satisfies the problem when  $H_p$  is the problem Hamiltonian. Therefore, theoretically, the larger the value, the closer to the optimal value. According to (9) and (10)  $|\varphi\rangle$  can also be expressed as:

$$|\varphi\rangle = U_{H_0}(\beta)U_{H_p}(\gamma)|\varphi_0\rangle \quad (19)$$

where  $|\varphi_0\rangle$  is the initial bit of the qubit passing through the Hadamard gate, and the complete quantum circuit is shown in Fig. 2.

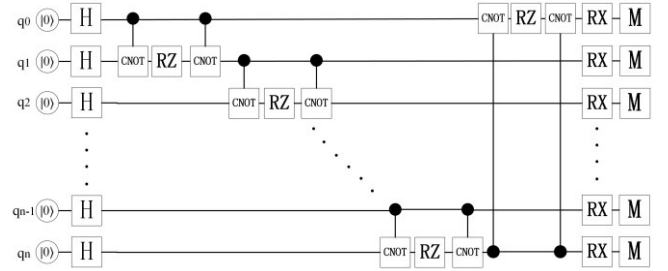


Fig. 2. This graph is a QAOA quantum circuit of  $n$  qubits. The circuit assumes that each vertex is connected by two edges.

### C. Applying QAOA on NOMA user pairing

To apply QAOA to NOMA user pairing, we need to abstract the NOMA user pairing system model into a weighted undirected graph, and the weight setting is determined by the objective function. This section describes how to apply QAOA to NOMA by dividing 4 users into two groups (where it is assumed that there are always two users in each group). The weights, as mentioned, are

$$\omega_{i,j} = 1 / \left| |h_i|^2 - |h_j|^2 \right| \quad (20)$$

where  $\omega$  is the weight,  $|h_i|^2$  is the channel gain from user  $i$  to the base station, and  $|h_j|^2$  is the channel gain from user  $j$  to the base station. Obviously  $\omega_{i,j} = \omega_{j,i}$ . QAOA can then be used as described in afore-mentioned Section III-C. Each step of the algorithm is as follows:

---

#### Algorithm 1 QAOA for User Pairing in NOMA

---

**Input:** user channel gain  $|h_k|^2, k \in \{1, 2, \dots, n\}$

**Output:** solution  $z$

**Initialization:**

Set  $\beta = 1, \gamma = 1$ .

for  $i = 1, 2, \dots, n$

for  $j = 1, 2, \dots, n$  &&  $j > i$

---

---

$\omega_{i,j} = 1/||h_i|^2 - |h_j|^2|$ , Calculate the weight of each edge

$H_\alpha = \omega_{i,j} * H_\alpha$ , Add weights to each sub-Hamiltonian

end

end

$H_p = \sum_{\alpha=1}^V H_\alpha$ , V is the set of edges. Calculate the problem Hamiltonian

**Iterations:**

Setting up quantum circuits according to the problem Hamiltonian  $H_p$

Measure and get the qubit state  $z = |\varphi\rangle$

Calculate the expected value of the Hamiltonian(loss function):  $LOSS = \langle \varphi | H_p | \varphi \rangle$

Use the classical optimizer to optimize the parameters  $\beta$  and  $\gamma$  so that the expected value LOSS is as large as possible.

**end**

Return the global solution  $z$

---

The QAOA of Algorithm 1 was applied to a 4-user NOMA downlink user pairing. In order to accommodate more users, an improved-QAOA is derived in the next section, which enables the system to obtain more groups to meet the requirements of NOMA downlink user pairing.

#### IV. IMPROVED-QAOA AND ITS APPLICATION

We use a matching matrix D to represent the grouping of bit strings. For example, in the original QAOA algorithm, the matching matrix D can be represented as follows:

$$D = \begin{bmatrix} -1 & 1 \\ 1 & -1 \end{bmatrix} \quad (21)$$

where the number of rows in this matrix represents the number of bit states provided by one vertex, and the number of columns represents the number of bit states provided by the other vertex. Therefore, any element in this matrix represents the weight of the vertices represented by the row and column in the same cluster. (21) can be expanded column-wise into a diagonal matrix H, which is the Hamiltonian of a clause, as:

$$H = \begin{bmatrix} -1 & 0 & 0 & 0 \\ 0 & 1 & 0 & 0 \\ 0 & 0 & 1 & 0 \\ 0 & 0 & 0 & -1 \end{bmatrix} \quad (22)$$

where the element on the diagonal line in (22) represents the energy of the qubit string corresponding to the element.

In the improved-QAOA, more qubits have been used to describe the state of a vertex in order to obtain more clusters. As an example, two qubits were used to describe a vertex, where the vertex now has four states, namely 00, 01, 10, and 11, and the corresponding matrix D is described by:

$$D = \begin{bmatrix} -1 & 1 & 1 & 1 \\ 1 & 1 & 1 & 1 \\ 1 & 1 & 1 & 1 \\ 1 & 1 & 1 & -1 \end{bmatrix} \quad (23)$$

where it can also be expanded column-wise as in (21) to get the Hamiltonian H:

$$H = \text{diag}(-1,1,1,1,1, -1,1,1,1,1, -1,1,1,1,1, -1) \quad (24)$$

For brevity, H is decomposed into H1, H2, H3, H4:

$$H = H_1 + H_2 + H_3 + H_4,$$

$$\begin{aligned} H_1 &= 0.5 * \text{diag}(1,1,1,1,1,1,1,1,1,1,1,1,1,1,1,1) \\ H_2 &= -0.5 * \text{diag}(1, -1, -1,1,1, -1, -1,1,1, -1, -1,1,1, -1, -1,1) \\ H_3 &= -0.5 * \text{diag}(1,1, -1, -1,1,1, -1, -1,1,1, -1, -1,1,1, -1, -1) \\ H_4 &= -0.5 * \text{diag}(1, -1,1, -1,1, -1,1, -1,1, -1,1, -1,1, -1,1, -1) \end{aligned} \quad (25)$$

Then from (10) and (25), the problem Hamiltonian Operator can be derived as:

$$U_{H_p} = e^{-i\theta(H_1+H_2+H_3+H_4)} = U_{p1} + U_{p2} + U_{p3} + U_{p4} \quad (26)$$

Using four qubits as an example, the quantum circuit described by (26) is illustrated in Fig. 3 where we used two qubits to describe a vertex, so that there are 16 possible groups of two vertices. As shown in Fig. 4, only four bit strings (0000, 0101, 1010, 1111) are not our desired results, and the rest are correct solutions.

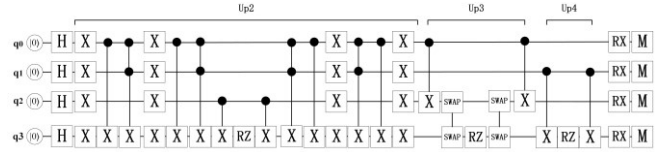


Fig. 3. This figure is the quantum circuit of the improved QAOA algorithm. It uses 4 qubits, each of which represents a vertex in a bipartite graph. In the figure, Up2, Up3, and Up4 respectively represent the operations corresponding to the three sub-Hamiltonians.

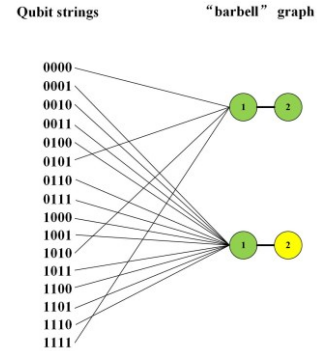


Fig. 4. The figure reflects the matching relationship between the qubit string and the barbell graph.

As shown on the left side in Fig.4, we use the first two qubits of the qubit string to represent the first vertex in the right graph, and the last two qubits to represent the second vertex in the right graph. On the left side of the figure, we use the first two qubits of the qubit string to represent the first vertex in the right image, and the last two qubits to represent the second vertex in the right image. When the colors of the vertices are the same, it means that the vertices are in the same cluster, and when they are different, they are in different clusters

In this case, since we can color vertices with four colors, but two vertices only use at most two colors, the remaining unused colors open up the possibility to support more vertices. After analysis, the number of qubits used by each vertex  $N_v$  and the maximum number of groups  $N_g$  (maximum coloring types) satisfy the following relationship:

$$N_g = 2^{N_v} \quad (27)$$

Therefore, up to 4 groups can be supported in this example. If more groups are needed, more qubits can be used to represent a vertex, and the quantum circuit will then adjust

accordingly. The improved-QAOA proposed in this section can obtain more clusters and improve the system throughput of QAOA in NOMA user pairing.

## V. RESULTS

In this section, we first visualize the expected value of the improved-QAOA and then compare the sum rate of the different algorithms under 8-user NOMA. Fig. 5 shows the landscape of the expectation values for a depth of  $p = 1$  circuits with two parameters  $\gamma_1$  and  $\beta_1$ , where the expectation values of  $\text{LOSS}(\gamma_1, \beta_1)$  are shown in (18) and (19). We see that in Fig. 5 the expectation values are non-convex in terms of  $\gamma_1$  and  $\beta_1$ , since there are multiple local minima. This poses a challenge to the classical optimization part of QAOA.

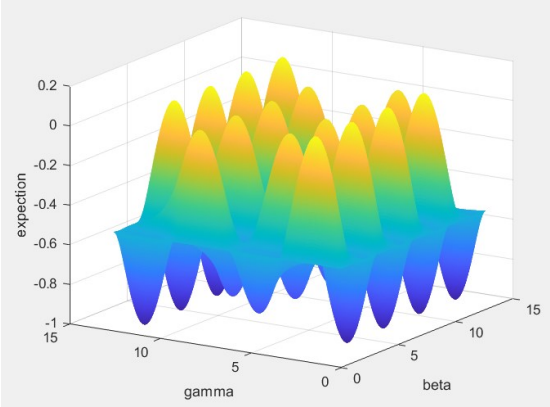


Fig. 5. The expectation value of I-QAOA,  $p=1$ .

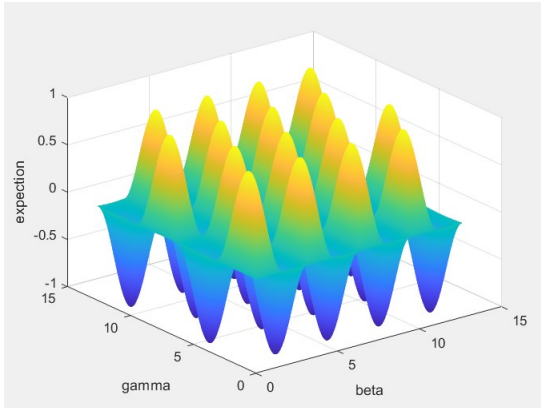


Fig. 6. The expectation value of QAOA,  $p=1$ .

In addition, we give the expected value of the QAOA landscape in Fig. 6. A comparison with QAOA shows that the number of minima of the expected values of I-QAOA, although the same, is half of the minimum value of QAOA. That is, in the classical optimization process, QAOA is able to be closer to the minimum if both algorithms fall into local minima at the same time. That is, using I-QAOA will be a greater challenge for classical optimizers than using QAOA.

The performances of using the original QAOA and the improved-QAOA are evaluated where an average results of 50 random simulations have been analyzed. In QAOA we need to use the optimizer to optimize the parameters of  $\alpha$  and  $\beta$ . Because Adma optimizer has the advantages of both Adagrad optimizer and RMSProp optimizer, and it only needs a small amount of memory, so we have chosen Adma optimizer as the optimizer of the classical part of QAOA algorithm. The NOMA power allocation coefficient in this paper adopts a

fixed power allocation which satisfies the following constraints:

$$\begin{aligned} \sum_{i=1}^N \alpha_i &= 1 \\ \alpha_{i+1} &= \frac{3}{4} * \alpha_i, i \in \{1, 2, \dots, N-1\} \\ \alpha_1 &= \frac{3}{4}, \alpha_N = 1 - \sum_{i=1}^{N-1} \alpha_i \end{aligned} \quad (28)$$

where  $N$  represents the number of users superimposed on a sub-bandwidth. The power coefficients are allocated to users according to their distances to the BS in descending order. Even so,  $\alpha_1$  represents the nearest user and  $\alpha_N$  represents the farthest user, to the BS, respectively. Other simulation parameters are shown in Table I. In addition, brute-force enumeration method is also used to determine user pairing. It took a lot of time to find the corresponding solution of all matching schemes and select the maximum value as the theoretical optimal solution, which is compared with other methods.

TABLE I. PARAMETER SETTINGS

Stochastic simulation times	50
Number of optimizer iterations	120
The number of users	8
Number of transmitted signals	$10^5$ (bits)
Distance from the user to the base station	1~1000 (m)
Total system bandwidth	$20 * 10^6$ (Hz)
Channel fading	Rayleigh
Optimizer	AdamOptimizer

In Fig. 7, the average sum rate per pair of Improved-QAOA, QAOA, random user pairing, and an Enumeration search algorithm with respect to different transmit power (hence SNR) is compared. It can clearly be seen that QAOA has comparable performance when compared with the random algorithm, although it is slightly better. When the transmit power is 1 dbm, QAOA can reach 14.969bit/s/Hz, and random algorithm can reach 14.790bit/s/Hz. When the transmit power is increased to 20dbm, the QAOA can reach 33.697bit/s/Hz, and the random algorithm can reach 33.633bit/s/Hz. The improved-QAOA, on the other hand, is superior to the above-mentioned two algorithms in the range of transmit power. When the transmit power is 1dbm and 20dbm, the I-QAOA achieves a rate of 26.343bit/s/Hz and 51.642bit/s/Hz, respectively, which is closer to the theoretical optimal value of 29.200bit/s/Hz and 54.098bit/s/Hz obtained by the brute-force enumeration method.

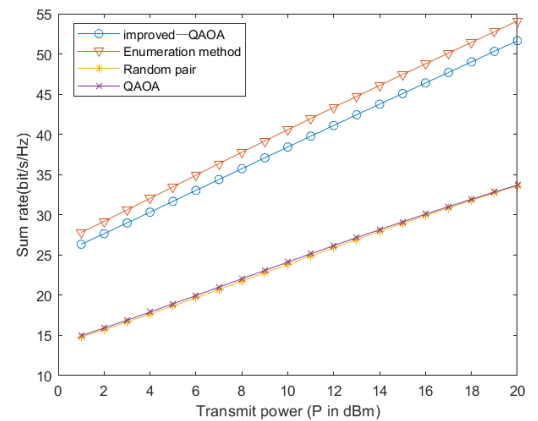


Fig. 7. Average sum rate per pair comparisons of Improved-QAOA, QAOA, random user pairing, and an Enumeration search algorithm.(All of the above scenarios are based on 8 users)

## VI. CONCLUSION

In this work, the original QAOA has been applied to NOMA user pairing for the first time. The results are compared with that of the random pairing algorithm where it shows that QAOA achieved slightly better results than the random pairing algorithm. Therefore, the feasibility of QAOA in NOMA user pairing has been proven. However, as the number of users increases, QAOA algorithm will cause more users to superpose, which will reduce the overall system rate and increase the complexity of SIC. Therefore, an improved QAOA has been proposed, which can set the number of clusters freely to obtain a higher total system rate. Then we compare the improved QAOA with the above two algorithms. The solution of the improved QAOA algorithm is obviously superior to the above two algorithms, but it is slightly lower than the optimal solution obtained by the enumeration method.

After analysis, we found in the QAOA simulation that the classical optimizer has at least the following two problems: 1. The optimizer based on the principle of gradient descent is used to optimize the parameters, and the convergence speed of the optimizer is not good. 2. We find that the loss function to be optimized is a multilevel valued function, and the optimizer may converge to a local minimum instead of a global minimum. In future research, using artificial intelligence algorithms to optimize parameters may yield better solutions.

## REFERENCES

- [1] Z. Ding, X. Lei, G. K. Karagiannidis, R. Schober, J. Yuan and V. K. Bhargava, "A Survey on Non-Orthogonal Multiple Access for 5G Networks: Research Challenges and Future Trends," in *IEEE Journal on Selected Areas in Communications*, vol. 35, no. 10, pp. 2181-2195, Oct. 2017, doi: 10.1109/JSAC.2017.2725519.
- [2] Mahmoud Aldababsa, Mesut Toka, Selahattin Gökçeli, Güneş Karabulut Kurt, Oğuz Kucur, "A Tutorial on Nonorthogonal Multiple Access for 5G and Beyond", *Wireless Communications and Mobile Computing*, vol. 2018, Article ID 9713450, 24 pages, 2018. <https://doi.org/10.1155/2018/9713450>
- [3] S. M. R. Islam, N. Avazov, O. A. Dobre and K. -s. Kwak, "Power-Domain Non-Orthogonal Multiple Access (NOMA) in 5G Systems: Potentials and Challenges," in *IEEE Communications Surveys & Tutorials*, vol. 19, no. 2, pp. 721-742, Secondquarter 2017, doi: 10.1109/COMST.2016.2621116.
- [4] L. Dai, B. Wang, Y. Yuan, S. Han, I. Chih-lin and Z. Wang, "Non-orthogonal multiple access for 5G: solutions, challenges, opportunities, and future research trends," in *IEEE Communications Magazine*, vol. 53, no. 9, pp. 74-81, September 2015, doi: 10.1109/MCOM.2015.7263349.
- [5] Z. Ding, Z. Yang, P. Fan and H. V. Poor, "On the Performance of Non-Orthogonal Multiple Access in 5G Systems with Randomly Deployed Users," in *IEEE Signal Processing Letters*, vol. 21, no. 12, pp. 1501-1505, Dec. 2014, doi: 10.1109/LSP.2014.2343971.
- [6] Z. Ding, P. Fan and H. V. Poor, "Impact of User Pairing on 5G Nonorthogonal Multiple-Access Downlink Transmissions," in *IEEE Transactions on Vehicular Technology*, vol. 65, no. 8, pp. 6010-6023, Aug. 2016, doi: 10.1109/TVT.2015.2480766.
- [7] Q. -V. Pham, T. Huynh-The, M. Alazab, J. Zhao and W. -J. Hwang, "Sum-Rate Maximization for UAV-Assisted Visible Light Communications Using NOMA: Swarm Intelligence Meets Machine Learning," in *IEEE Internet of Things Journal*, vol. 7, no. 10, pp. 10375-10387, Oct. 2020, doi: 10.1109/JIOT.2020.2988930.
- [8] H. Zhang, M. Feng, K. Long, G. K. Karagiannidis and A. Nallanathan, "Artificial Intelligence-Based Resource Allocation in Ultradense Networks: Applying Event-Triggered Q-Learning Algorithms," in *IEEE Vehicular Technology Magazine*, vol. 14, no. 4, pp. 56-63, Dec. 2019, doi: 10.1109/MVT.2019.2938328.
- [9] X. Diao, J. Zheng, Y. Wu and Y. Cai, "Joint Computing Resource, Power, and Channel Allocations for D2D-Assisted and NOMA-Based Mobile Edge Computing," in *IEEE Access*, vol. 7, pp. 9243-9257, 2019, doi: 10.1109/ACCESS.2018.2890559.
- [10] L. Zhu, J. Zhang, Z. Xiao, X. Cao, D. O. Wu and X. -G. Xia, "Joint Tx-Rx Beamforming and Power Allocation for 5G Millimeter-Wave Non-Orthogonal Multiple Access Networks," in *IEEE Transactions on Communications*, vol. 67, no. 7, pp. 5114-5125, July 2019, doi: 10.1109/TCOMM.2019.2906589.
- [11] H. A. Ghani, A. A. Hamzah, M. A. Salem, A. A. Ahmed, A. A. Aziz and A. Azizan, "Ant-Colony Optimization for 5G NOMA User Grouping," 2020 IEEE International RF and Microwave Conference (RFM), 2020, pp. 1-4, doi: 10.1109/RFM50841.2020.9344788.
- [12] T. Sefako and T. Walingo, "Application of Biological Resource Allocation Techniques to SCMA NOMA Networks," 2019 IEEE AFRICON, 2019, pp. 1-7, doi: 10.1109/AFRICON46755.2019.9133767.
- [13] Z. Sheng, X. Su and X. Zhang, "A Novel Power Allocation Method for Non-orthogonal Multiple Access in Cellular Uplink Network," 2017 International Conference on Intelligent Environments (IE), 2017, pp. 157-159, doi: 10.1109/IE.2017.17.
- [14] Ö. F. Gemici, F. Kara, I. Hokelek, G. K. Kurt and H. A. Çırpan, "Resource allocation for NOMA downlink systems: Genetic algorithm approach," 2017 40th International Conference on Telecommunications and Signal Processing (TSP), 2017, pp. 114-118, doi: 10.1109/TSP.2017.8075948.
- [15] J. Choi and J. Kim, "A Tutorial on Quantum Approximate Optimization Algorithm (QAOA): Fundamentals and Applications," 2019 International Conference on Information and Communication Technology Convergence (ICTC), 2019, pp. 138-142, doi: 10.1109/ICTC46691.2019.8939749.
- [16] Haibin Wang, Jiaojiao Zhao, Bosi Wang, Lian Tong, "A Quantum Approximate Optimization Algorithm with Metalearning for MaxCut Problem and Its Simulation via TensorFlow Quantum", *Mathematical Problems in Engineering*, vol. 2021, Article ID 6655455, 11 pages, 2021. <https://doi.org/10.1155/2021/6655455>
- [17] E. Farhi, J. Goldstone, and S. Gutmann, "A quantum approximate optimization algorithm," arXiv preprint arXiv:1411.4028, 2014.
- [18] Y. Fu, L. Salaün, C. W. Sung and C. S. Chen, "Subcarrier and Power Allocation for the Downlink of Multicarrier NOMA Systems," in *IEEE Transactions on Vehicular Technology*, vol. 67, no. 12, pp. 11833-11847, Dec. 2018, doi: 10.1109/TVT.2018.2875601.
- [19] M. Yang, F. Gao, G. Wu, W. Dai and F. Shuang, "A Tutorial on Quantum Approximate Optimization Algorithm for Maximum Independent Set Problem," 2021 40th Chinese Control Conference (CCC), 2021, pp. 6317-6322, doi: 10.23919/CCC52363.2021.9550042
- [20] M. A. Ghonaimy, "An overview of Quantum Information Systems," 2013 8th International Conference on Computer Engineering & Systems (ICCES), 2013, pp. xx-xxxii, doi: 10.1109/ICCES.2013.6707155.